Floating electrode optoelectronic tweezers: Light-driven dielectrophoretic droplet manipulation in electrically insulating oil medium

Sungyong Park,[1] Chenlu Pan,[1] Ting-Hsiang Wu,[2] Christoph Kloss,[3] Sheraz Kalim,[4] Caitlin E. Callahan,[4] Michael Teitell,[4] and Eric P. Y. Chiou[1,a)]
[1]*Department of Mechanical and Aerospace Engineering, University of California at Los Angeles (UCLA), 48-121 ENG. IV, 420 Westwood Plaza, Los Angeles, California 90095-1597, USA*
[2]*Department of Electrical Engineering, UCLA, 48-121 ENG. IV, 420 Westwood Plaza, Los Angeles, California 90095-1597, USA*
[3]*Institute of Fluid Mechanics and Heat Transfer, Johannes Kepler University of Linz, Altenbergerstraße 69, 4040 Linz, Austria*
[4]*Department of Pathology, California NanoSystems Institute, the Center for Cell Control, Broad Institute for Regenerative Medicine and Stem Cell Research, and Jonsson Comprehensive Cancer Center, UCLA, 675 Charles E. Young Dr. South, MRL 4-762, Los Angeles, California 90095-1732, USA*

(Received 28 November 2007; accepted 15 March 2008; published online 14 April 2008)

We report an optical actuation mechanism, floating electrode optoelectronic tweezers (FEOET). FEOET enables light-driven transport of aqueous droplets immersed in electrically insulating oil on a featureless photoconductive glass layer with direct optical images. We demonstrate that a 681 μm de-ionized water droplet immersed in corn oil medium is actuated by a 3.21 μW laser beam with an average intensity as low as 4.08 $\mu W/mm^2$ at a maximum speed of 85.1 μm/s on a FEOET device. FEOET provides a promising platform for massively parallel droplet manipulation with optical images on low cost, silicon-coated glass. The FEOET device structure, fabrication, working principle, numerical simulations, and operational results are presented in this letter. © *2008 American Institute of Physics*. [DOI: 10.1063/1.2906362]

Droplet-based microfluidic systems have attracted significant interest for their potential utility in high throughput chemical and biological screening.[1–5] Using a multiphase flow focusing device, tens of thousands of highly uniform, isolated aqueous droplets can be generated in immiscible oil within seconds. Applications such as fluorescent detection of millisecond chemical kinetics,[6] laser Raman spectroscopic probing,[7] and polymerase chain reactions for high throughput DNA amplification[8] have been demonstrated using droplet-based microfluidic devices. One challenge associated with a droplet-based microfluidic system is the difficulty in achieving active control of individual droplets confined in microchannels being driven by a continuous oil flow.[2–6] It has been shown that multiple droplets can be individually addressed in an open oil chamber using physically patterned electrodes, although complex wiring and interconnection issues arise for addressing numerically large droplet arrays.[9,10] To solve this problem, a microfluidic device integrating a high voltage complementary metal-oxide semiconductor driving circuit recently achieved active and parallel droplet control. However, this approach increases the fabrication cost of microfluidic devices, which are often preferred to be disposable.[11]

Alternatively, a light-induced manipulation mechanism has been widely investigated to solve the wiring issues that arise for controlling a large array of electrodes.[12–15] For example, optoelectronic tweezers (OET) has recently been shown to manipulate single cells and microscopic particles sandwiched between an indium tin oxide electrode and a photoconductive electrode created by direct optical images.[15] However, due to impedance matching, it is difficult to modulate the electric field strength in electrically insulating mediums, such as oils used in two-phase droplet-based microfluidic systems, on an OET device since all of the applied voltage drops across the oil layer even without light illumination.

In this letter, we present an optically actuated droplet manipulation mechanism called floating electrode optoelectronic tweezers, FEOET, to enable optical modulation of the electric field in electrically insulating oils, which is required to create dielectrophoretic (DEP) forces for aqueous droplet actuation.

A schematic cross-sectional view of the FEOET device is illustrated in Fig. 1. The fabrication is implemented by depositing two *a*-Si:H layers (0.5 μm undoped and 0.1 μm n^+) on a glass substrate. Two aluminum electrodes separated by a 1 cm gap are deposited at the two edges of the device using a lift-off method enabling electrical contact. The n^+ *a*-Si:H layer not covered by Al electrodes is etched away using reactive ion etcher. The remaining covered n^+ *a*-Si:H layer reduces the electrical resistance between the Al electrodes and the undoped *a*-Si:H layer. An open polydimethylsiloxana (PDMS) chamber, housing aqueous droplets immersed in a corn oil medium, is fixed on top of the undoped *a*-Si:H layer.

A dc bias is applied to the two aluminum electrodes to provide a lateral electric field across the whole device in both

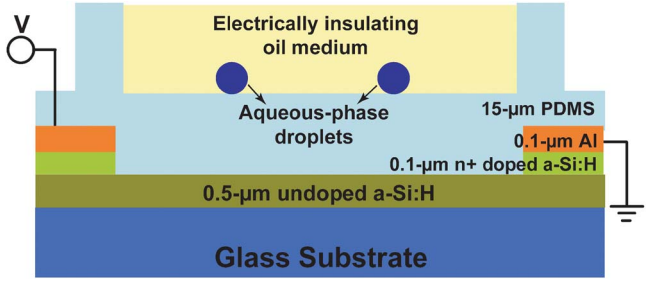

FIG. 1. (Color online) Schematic cross-sectional view of the FEOET device.

a)Electronic mail: pychiou@seas.ucla.edu.

 © 2008 American Institute of Physics
Author complimentary copy. Redistribution subject to AIP license or copyright, see http://apl.aip.org/apl/copyright.jsp

the oil and the undoped *a*-Si:H layers. In the absence of light illumination, the electric field uniformly drops across the oil and the silicon layers. When a light beam illuminates the undoped *a*-Si:H layer, photogenerated electron-hole pairs are created, which locally changes the photoconductivity. The originally uniform electric field is strongly perturbed near the illuminated area, resulting in two strong electric field regions near the two edges of the illuminated area parallel to the field direction and a weak field region in the middle of the illuminated area. This effect is similar to the field induced dipole on a metal ball in a uniform electric field, except that the electric dipole is induced by a light-patterned virtual electrode on a two-dimensional surface. The perturbed field penetrates into the oil layer, which creates nonuniformity of the electric fields necessary for DEP manipulation in the electrically insulating oil.

Since the aqueous droplets are much more conductive than the surrounding electrically insulating oil, an electric dipole is also induced on each droplet under the application of a lateral electric field. Even though a highly nonuniform electric field is induced around a droplet, there is no DEP force actuation on the droplet since the balanced electric field distribution around the droplet results in a zero net force. However, when a light beam illuminates near the edge of the droplet on the undoped *a*-Si:H layer, it creates a light-patterned virtual electrode which decreases the electric field strength at the illuminated side of the droplet. This breaks the originally balanced electric field pattern around a droplet and results in a nonzero net positive DEP force, which drives the droplet away from the light beam to the strong electric field region.

This working mechanism is verified by three-dimensional (3D) simulated results of electric field distribution calculated using finite-element software (COMSOL MULTIPHYSICS 3.2). To reduce the simulation time, the device is simplified to the following layers: 5 μm *a*-Si:H, 20 μm PDMS, and 500 μm oil medium. A 300 V dc is biased at the two end planes along the *x* direction, and a 300 μm diameter aqueous droplet is immersed in a 2×2 mm^2 oil environment on top of the thin PDMS layer. The dark conductivity of the homogeneous *a*-Si:H layer is assumed 10^{-8} S/m and the optical illumination is assumed to a full width at half maximum to create a Gaussian photoconductivity distribution with its peak conductivity of 10^{-4} S/m and spot size of 100 μm.

Figure 2 shows the 3D numerical simulations of the electric field distribution under the illumination of a circular light beam. The electric strength at the center of the illuminated area greatly decreases, while the field strength at the two edges along the electric field direction is enhanced. The largest electric field gradient exists near the *a*-Si:H surface as shown in Fig. 2(b) and the field perturbation can penetrate into the nearby electrically insulating oil layer as shown in Fig. 2(c), which can be applied to actuate aqueous droplets via DEP forces.

Figure 3 shows the numerical simulations of the electric field distribution when an ionic aqueous droplet is loaded into the oil environment. A symmetrical electric field distribution is developed around a droplet, owing to the droplet induced electric dipole. Such a balanced electric field pattern produces zero net DEP force on a droplet and so no movement occurs [Fig. 3(a)]. In the presence of light beam illumination at the edge of a droplet, the electric field strength at

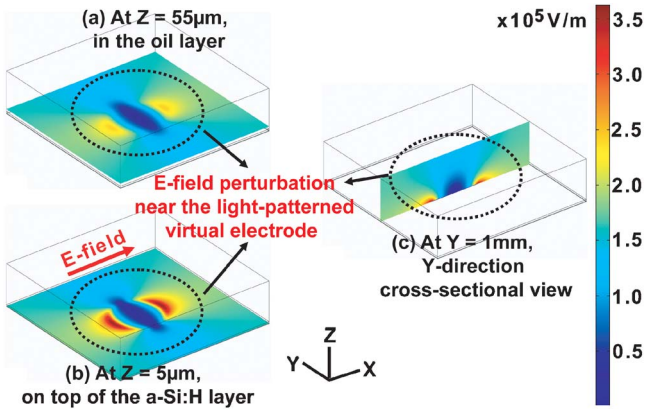

FIG. 2. (Color online) 3D numerical simulation results of the electric field distribution. (b) The light-patterned virtual electrode perturbs the e-field distribution in the *a*-Si:H layer. (a) This e-field perturbation is penetrated into an electrically insulating oil layer. (c) The electric field perturbation is developed in *y*-direction cross-sectional view.

the illuminated side is strongly attenuated, breaking the originally balanced field pattern and giving rise to a net positive DEP force moving the droplet away from the light beam [Fig. 3(b)]. The 3D electric field strength distributions on the surface of a droplet are shown in the bottom two plots in Figs. 3(a) and 3(b) to demonstrate the significant difference in the field patterns with and without light illumination.

The DEP force on a particle is usually estimated using $F=(p\nabla)E$, where p is the induced dipole and E is the electric field.[16] A good approximation is obtained only when the particle size is much smaller than the gradient of the electric field, criteria that is not satisfied to estimate the DEP force on a droplet whose size is comparable to the light induced electric field gradient. To precisely calculate the light-induced DEP force exerted on a droplet, we integrate the Maxwell stress tensor over the whole droplet surface,

$$F_{\mathrm{DEP}}=\int_{\mathrm{surface}}\frac{1}{2}\varepsilon E^2 ds. \tag{1}$$

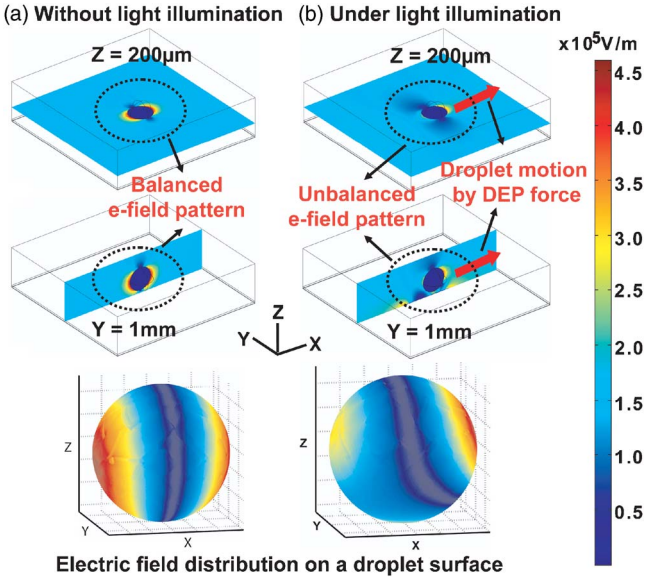

FIG. 3. (Color online) Numerical simulations of the electric field distribution around an aqueous droplet. (a) Without light illumination, the balanced electric field distribution is exhibited around an electric dipole of a droplet. (b) Optical illumination creates an unbalanced electric field distribution near a droplet. The DEP force drives a droplet away from the illuminated spot.

Author complimentary copy. Redistribution subject to AIP license or copyright, see http://apl.aip.org/apl/copyright.jsp

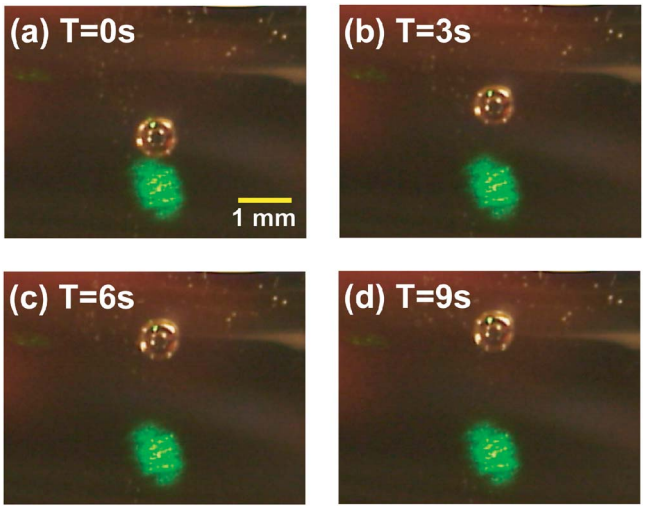

FIG. 4. (Color online) Experimental results of the light-actuated de-ionized water droplet movement in corn oil medium.

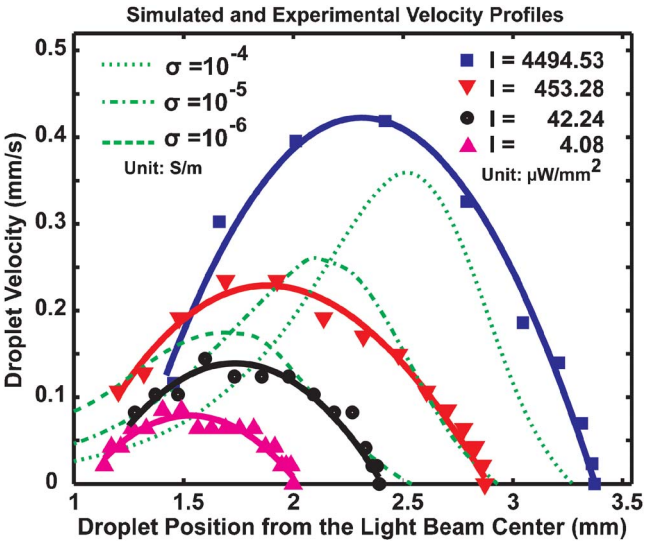

FIG. 5. (Color online) Simulated and experimental droplet velocity profiles depending on the droplet position at various light intensities.

The electric field strength acting on all infinitesimal areas of a droplet surface are calculated using the 3D finite element numerical simulation data and their integrations are completed over the entire droplet surface using the spherical coordinates. Based on the droplet situation shown in Fig. 3(b), where the center of the droplet is at 100 μm away from the center of the light beam along the x direction, the optically induced DEP force exerted on the droplet is estimated as $F_{\mathrm{DEP}}=[2.60,-0.01,1.12]\times10^{-8}$ N. This estimated DEP force predominates in the x and z directions, meaning that the light-induced virtual electrode raises a droplet and pushes it away from the illuminated spot along the direction of electric field. The theoretical value of the y direction force should be zero due to symmetry, and the value in the simulation data comes from numerical errors due to limited computation power for 3D simulation.

Light-induced droplet actuation has been experimentally demonstrated on the FEOET device. For the experimental setup, we utilize a laser beam (3.53 mW at 532 nm) with a 1 mm output spot size, a charge-coupled device camera (Sony, DFW-SX910) and metallic neutral density filters (Newport). Figure 4 shows video snapshots of a de-ionized water droplet, immersed in corn oil medium, being repelled by a light beam as predicted in our simulation results. Figure 5 shows both simulated and experimental velocity profiles depending on the droplet positions at various light intensities. For simulated data, we assume the photoconductivity in the a-Si:H layer is linearly proportional to a circular light beam with a Gaussian intensity profile. The simulated velocity profiles are determined by the force balance between the DEP and the Stokes' drag. Both simulated and experimental plots show that the maximum droplet velocity and the position where it occurs increase as the light intensity. The experimental data also confirms that a light beam with a higher intensity gives a larger actuation range. A maximum droplet speed of 418.6 μm/s has been achieved on a 748 μm droplet with a light intensity of 4.49 mW/mm^2. By reducing the light intensity to 4.08 μW/mm^2, FEOET still allows optical actuation of a 681 μm droplet at a maximum speed of 85.1 μm/s. The maximum velocity is limited by the maximum voltage that can be applied to FEOET devices. The electric field strength applied here is 600 V/cm. Applying a higher voltage could give larger DEP forces and faster droplet motion.

In conclusion, we report a droplet manipulation mechanism FEOET, which enables optical actuation of aqueous droplets in electrically insulating media on a plain amorphous silicon coated glass device. FEOET allows light-patterned virtual electrodes to perturb a uniform electric field distribution, breaking an originally symmetric electric field pattern around a droplet for DEP actuation. FEOET promises a large-scale droplet manipulation platform for parallel droplet processing on a low cost substrate using flexible optical addressing.

This project is supported by the NSF Career Award (ECCS-0747950), by the NIH Roadmap for Medical Research Nanomedicine Initiative PN2EY018228, and in part by NIH Grants Nos. CA90571 and CA107300.

[1]D. Albrecht, G. Underhill, A. Mendelson, and S. Bhatia, Lab Chip **7**, 702 (2007).
[2]T. Tan, K. Hettiarachchi, M. Siu, Y. Pan, and A. P. Lee, J. Am. Chem. Soc. **128**, 5656 (2006).
[3]L. Li, J. Boedicker, and R. Ismagilov, Anal. Chem. **79**, 2756 (2007).
[4]D. L. Chen, L. Li, S. Reyes, D. N. Adamson, and R. F. Ismagilov, Langmuir **23**, 2255 (2007).
[5]S. Xu, Z. Nie, M. Seo, P. Lewis, E. Kumacheva, H. Stone, P. Garstecki, D. Weibel, I. Gitlin, and G. Whitesides, Angew. Chem. **117**, 734 (2005).
[6]H. Song and R. Ismagilov, J. Am. Chem. Soc. **125**, 14613 (2003).
[7]G. Cristobal, L. Arbouet, F. Sarrazin, D. Talaga, J. Bruneel, M. Joanicot, and L. Servant, Lab Chip **6**, 1140 (2006).
[8]M. Curcio and J. Roeraade, Anal. Chem. **75**, 1 (2003).
[9]J. Schwartz, J. Vykoukal, and P. Gascoyne, Lab Chip **4**, 11 (2004).
[10]C. Lee, G. Sui, A. Eli, C. Shu, Y. Shin, A. Dooley, J. Huang, A. Daridon, P. Wyatt, D. Stout, H. Kolb, O. Witte, N. Satyamurthy, J. Heath, M. Phelps, S. Quake, and H. Tseng, Science **310**, 1793 (2005).
[11]N. Manaresi, A. Romani, G. Medoro, L. Altomare, A. Leonardi, M. Tartagni, and R. Guerrieri, IEEE J. Solid-State Circuits **38**, 2297 (2003).
[12]A. Ohta, A. Jamshidi, J. Valley, H.-Y. Hsu, and M. Wu, Appl. Phys. Lett. **91**, 074103 (2007).
[13]A. Ohta, P. Chiou, H. Phan, S. Sherwood, J. Yang, A. Lau, H. Hsu, A. Jamshidi, and M. Wu, IEEE J. Sel. Top. Quantum Electron. **13**, 235 (2007).
[14]P. Chiou, H. Moon, H. Toshiyoshi, C. Kim, and M. Wu, Sens. Actuators, A **104**, 222 (2003).
[15]P. Y. Chiou, A. T. Ohta, and M. C. Wu, Nature (London) **436**, 370 (2005).
[16]T. B. Jones, *Electromechanics of Particles* (Cambridge University Press, Cambridge, 1995).

Author complimentary copy. Redistribution subject to AIP license or copyright, see http://apl.aip.org/apl/copyright.jsp